Flow speed of the ablation vapors generated during laser drilling of CFRP with a continuous-wave laser beam

S. Faas[1] · C. Freitag[1] · S. Boley[1] · P. Berger[1] · R. Weber[1] · T. Graf[1]

Abstract The hot plume of ablation products generated during the laser drilling process of carbon fiber reinforced plastics (CFRP) with a continuous-wave laser beam was analyzed by means of high-speed imaging. The formation of compression shocks was observed within the flow of the evaporated material, which is an indication of flow speeds well above the local speed of sound. The flow speed of the hot ablation products can be estimated by analyzing the position of these compression shocks. We investigated the temporal evolution of the flow speed during the drilling process and the influence of the average laser power on the flow speed. The flow speed increases with increasing average laser powers. The moment of drilling through the material changes the conditions for the drilling process and was confirmed to influence the flow speed of the ablated material. Compression shocks can also be observed during laser cutting of CFRP with a moving laser beam.

1 Introduction

During laser processing of carbon fiber reinforced plastics (CFRP), the material is mostly removed in a gaseous phase since both components have no liquid phase [1]. The composition of the gaseous emissions is reported in [2]. Several components contained in the hot ablation plume, such as bisphenol A or CO are potentially hazardous. Therefore, they must be evacuated reliably from the processing area.

To guarantee a reliable evacuation of the gaseous emissions, their flow speeds have to be known. Furthermore, a strong interaction between the hot plume of ablation products and the processed material has been reported in [3]. The plume can lead to a bulged cutting edge when laser cutting carbon fiber preforms which degrades the quality of the cut [3]. An interaction between the ablation plume and the carbon fibers can also be observed when laser cutting CFRP with a considerable matrix evaporation zone (MEZ). In this case, the matrix material near the interaction zone is vaporized due to an extensive heat input as reported in [4–6]. In a large MEZ, the carbon fibers lose their fixation in the compound and can interact with fast-flowing ablation products. Measurements of the flow speed of the ablated material to investigate whether fast-flowing ablation products are responsible for the bulging of the cutting edge were already reported in [3]. For this, the samples were placed on a weighing scale and the resulting force during laser cutting of carbon fiber preforms was measured. By measuring the downwards component of the resulting force, the momentum and, also, the average speed of the ablated material were determined as a mass-weighted average over all ablated particles. It was reported that the ablation products leave the interaction zone with average speeds ranging between 100 and 300 m/s.

The speed of ablated particles during laser processing of CFRP with a pulsed laser system delivering pulses with a duration of 20 ns is reported in [7]. The material was ablated by single shots on the material surface. Particles of carbon fibers that leave the interaction zone with speeds between 1700 and 6000 m/s were observed by means of high-speed imaging. Equally high speeds of the evaporated material are stated in [8]. In this case, the CFRP workpiece was also processed at the material surface with single pulses with a duration of 4 ps. The material vapor

S. Faas and C. Freitag contributed equally to this work.

✉ S. Faas
sebastian.faas@ifsw.uni-stuttgart.de

[1] Institut für Strahlwerkzeuge (IFSW), Universität Stuttgart, Pfaffenwaldring 43, 70569 Stuttgart, Germany

cloud was measured to propagate at speeds between 4500 and 5000 m/s. It is noticeable that there seems to be significant differences in the flow speed of the ablated material depending on the operating mode of the utilized laser system. To gain further insights on the flow of the ablated material, we exploited the gas dynamic properties of compressive shocks as a further approach to estimate the flow speeds of the ablation products generated during laser processing of CFRP with a continuous-wave laser. A high-speed camera was used to observe the compression shocks that are formed within the plume of ablation products during the process. The existence of compression shocks within the flow of the evaporated material already indicates flow speeds well above the local speed of sound.

2 Experimental setup

The experiments were performed with a continuous-wave laser having a wavelength of 1030 nm. The beam propagation factor was $M^2 \approx 15$. The maximum average laser power used for the presented experiments was 3.5 kW. The laser beam was focused on the surface of the work pieces with a focus diameter of about $d_f \approx 300$ µm. The beam was moved over the CFRP surface by a scanner system equipped with an F-Theta lens having a focal length of 163 mm. The CFRP samples were made from PAN-based carbon fibers in a quasi-isotropic arrangement with an epoxy resin as matrix material. The samples had a total thickness of 4.5 mm. The thickness of the individual layers was 0.28 mm each. The fiber volume content was about 55%.

The hot plume of ablation products generated during the ablation process was observed by means of a high-speed camera which was positioned at the side of the workpiece. A band-pass filter for a wavelength of 810 ± 10 nm

was placed in front of the camera to filter the laser wavelength and most of the process radiation. The plume was not illuminated; only the thermal emission of the plume was detected. The process was recorded with a rate of 7500 frames per second, the exposure time was set to 133.1 µs, and the resolution was 1024×1000.

3 Theory

The investigations concentrated on the drilling process to avoid the influence of a moving beam. The observation of a stable flow of the ablation products was, thus, possible. Single frames of the plume of ablation products generated during laser drilling are shown in Fig. 1. The left picture shows an image recorded 1.6 ms after the start of the drilling process with an average laser power of $P = 1$ kW. In the picture on the right, the material was drilled with an average laser power of 3.5 kW and the image was recorded 1.0 ms after the start of the process.

The surface of the workpiece is marked with a white line. The first compression shock can be detected at a distance x_M from the workpiece surface. The formation of compression shocks indicates a flow of material with supersonic speed and high pressure [9]. Usually, compression shocks are observed for an overexpanded flow through a nozzle. To the best of our knowledge, this is the first time compression shocks are used to determine the flow speed of the ablation vapors during processing of CFRP. In the case of laser drilling, the bore hole can be regarded as a nozzle opening. In Fig. 1a, an oblique compression shock and in Fig. 1b, a vertical compression shock can be seen. This vertical compression shock is commonly referred to as Mach disc. Depending on the conditions, it occurs when the pressure ratio $p_{t,D}/p_{atm}$ of the total pressure $p_{t,D}$ in the

Fig. 1 Side view of the ablation plume generated during laser drilling of CFRP with a continuous-wave laser. **a** $P = 1.0$ kW, recorded 1.6 ms after start of the drilling process, **b** $P = 3.5$ kW, recorded 1.0 ms after start of the drilling process. Additional process parameters: $\lambda = 1030$ nm, $df \approx 300$ µm, $M^2 = 15$, nonpolarized. Exposure time 133.1 µs
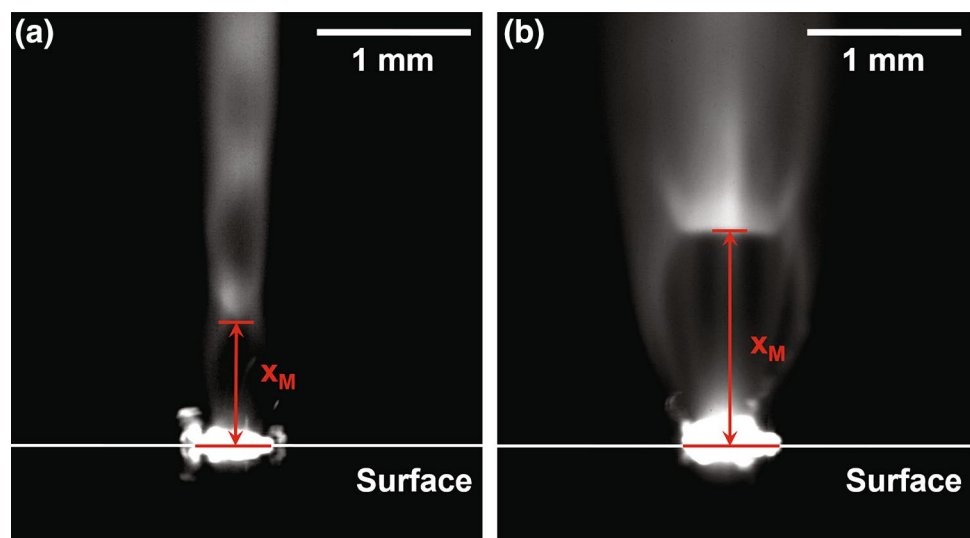
flow at the nozzle outlet and the ambient pressure p_{atm} is larger than 2–4 [9]. With an increasing pressure ratio, the Mach disc gets more pronounced. For $p_{t,D}/p_{atm} < 2$, oblique compression shocks are formed [9]. The flow speed of the evaporated material can be calculated if the distance x_M, the nozzle diameter D_N and the ambient pressure p_{atm} are known. The pressure ratio $p_{t,D}/p_{atm}$ at the nozzle outlet can be expressed by [9]:

$$\frac{p_{t,D}}{p_{atm}} = \left(\frac{x_M}{0.7 \cdot D_N}\right)^2. \tag{1}$$

The Mach number of the flow in the first compression shock is given by:

$$Ma = \sqrt{\frac{2}{\kappa - 1} \cdot \left[\left(\frac{p_{t,D}}{p_{atm}}\right)^{\frac{\kappa-1}{\kappa}} - 1\right]}, \tag{2}$$

where κ is the isentropic exponent. To calculate the flow speed

$$v = Ma \cdot c. \tag{3}$$

The local speed of sound

$$c = \sqrt{\frac{\kappa \cdot R \cdot T}{M}}, \tag{4}$$

must be known, whereby R is the universal gas constant, T is the temperature of the gas and M is the molar mass of the gas.

The ambient pressure in our case was supposed to be $p_{atm} = 1013$ mbar. The composition of the gaseous ablation products should be known to determine the isentropic exponent. The exact composition is not yet clear, but in [2], it was reported that CO is generated during laser processing of CFRP. In addition, the existence of C_2 and CN in the exhausting plume has been shown in [10]. Due to the several diatomic gases that are generated when CFRP is being processed with lasers, the isentropic exponent was assumed to be $\kappa = 1.4$. This is a typical value for most diatomic gases

at ambient temperature [9]. The universal gas constant is $R = 8{,}314$ J/mol K [6]. The molar mass of the evaporated material was averaged over the diatomic gases CO, C_2 and CN which leads to $M = 26.02$ g/mol. For average laser powers of 0.5, 0.8 and 1.0 kW and a laser beam moved with a feed rate of 0.1 m/s, but otherwise with process parameters identical to the ones specified above, the temperature (determined by fitting Planck's law to the emission spectrum of the plume) was found to be about 4000 K, independent of the average laser power. The nozzle diameter D_N, i.e. the diameter of the drilled holes, was measured by means of an optical microscope following the drilling process. During the drilling process, the real diameter of the drilling hole may be smaller than the measured diameter of the drilling hole leading to an unknown systematic error that was not taken into account. At different times of the drilling process, the distance x_M was obtained by analyzing single frames of the high-speed recordings of the process. For the calculation of v from Eq. (4), we have assumed an error of the isentropic exponent of $\Delta\kappa = 0.1$, an error of the molar mass of $\Delta M = 5.2$ g/mol, and an error of the plume's temperature of $\Delta T = 400$ K. For the measured nozzle diameter, we estimated an error of 5% of the measured value, and for the measured distance x_M, we estimated the error to be 10% of the measured value.

4 Experimental results

The pressure ratio and the flow speeds determined at different times after the start of the drilling process are shown in Fig. 2 for the different average laser powers of 1, 2 and 3.5 kW. Generally, the pressure ratio as well as the flow speed increase at the beginning of the drilling process until they reach a saturation value. For a certain period, the pressure ratio and the flow speed remain approximately constant. After this period, the pressure ratio and the flow speed decrease until no compression shocks can be observed anymore. The highest pressure ratio of about

Fig. 2 **a** Pressure ratio $p_{t,D}/p_{atm}$ and **b** flow speed in the first compression shock as a function of the drilling time for several average laser powers. Process parameters: $\lambda = 1030$ nm, $df \approx 300$ μm, $M^2 \approx 15$, nonpolarized, sample thickness: 4.5 mm
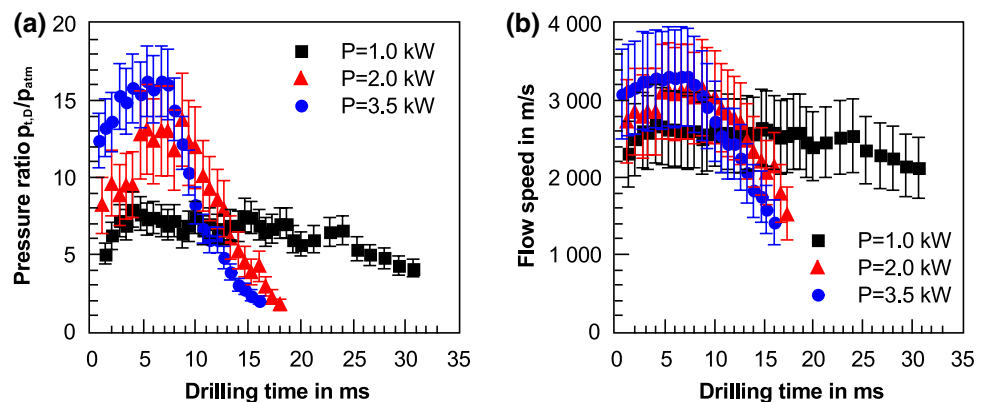
16 was measured for the maximum applied average laser power of 3.5 kW. The flow speed at the saturation level is higher for larger average laser powers. The period with approximately constant flow speed becomes shorter with larger average laser powers. The curves typically show a more or less distinct kink at which the flow speed starts to decrease significantly. As discussed later below, this kink is supposed to be related with the breakthrough of the laser beam through the material. The higher the cw laser power, the more distinct is the kink at which the flow speed decreases. At the laser powers of 3.5 and 2 kW, the kink in Fig. 2 is seen to occur at about 8 and 9 ms after the start of the drilling process, respectively. With 1 kW of laser power, this kink is less distinct and occurs approximately at 24 ms after the start of the drilling process.

The influence of the cw laser power on the flow speed of the evaporated material measured after a drilling time of $t_{Drill} = 5$ ms at which a stable flow state was reached is shown in Fig. 3. It can be seen that the flow speed of the evaporated material increases with higher cw laser power. As expected from basic energy considerations [11], according to which the evaporated volume is proportional to the absorbed laser power, the highest flow speed of about 3300 m/s was measured for the maximum applied average laser power of 3.5 kW.

To verify that the observed kink in the flow speed over time is caused by the breakthrough through the CFRP workpieces, the time of the breakthrough was determined for different average laser powers by means of photodiodes. One photodiode was placed on the top of the workpiece to detect the beginning of the drilling process; another was placed below the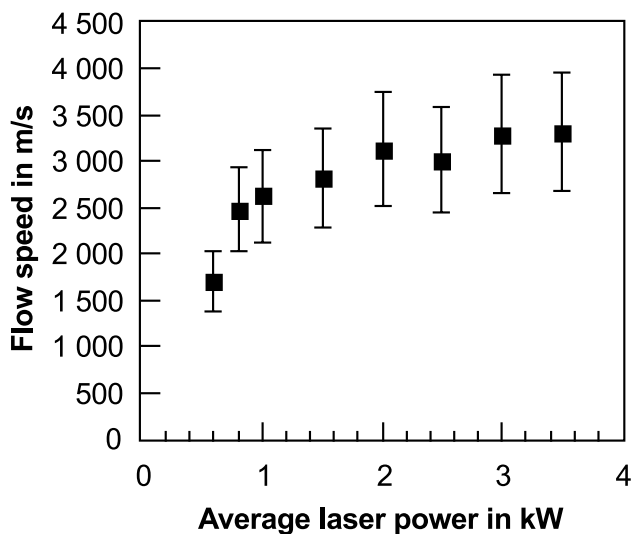 workpiece to detect the moment of breakthrough. Both photodiodes measured scattered light. For different laser powers, the required process time from the beginning of the drilling process to the moment of breakthrough is shown in Fig. 4 and compared to the times at which the flow speed of the ablated vapor starts to decrease significantly. The comparison was only possible for powers of 1 kW and above, as for lower powers, the compression shock vanishes before reaching the breakthrough (see also discussion of Fig. 2). But for the measurements with powers of 1 kW and higher, there is an excellent correlation between the moment of breakthrough and the process time at which the flow speed of the ablated vapor starts to decrease.

The relation seems plausible since the vaporized material can escape on both sides of the workpiece once this is drilled through. In addition, part of the laser radiation propagates through the material and no longer contributes to the removal of the material. This leads to a reduction of the volume of the evaporated material which again results in a lower pressure within the drilled hole. According to Eq. (2), a reduced pressure leads to lower flow speeds.

It should be noted that in the frame of this study, we did not determine whether the temperature of the vaporized material remains 4000 K after the moment of breakthrough or if it decreases. According to Eq. (3), a temperature reduction results in lower local speeds of sound which leads to a reduction of the flow speed according to Eq. (4). The flow speeds shown in Fig. 2 were calculated assuming a constant temperature $T = 4000$ K and, therefore, give an upper limit of the flow speeds after the moment of breakthrough.
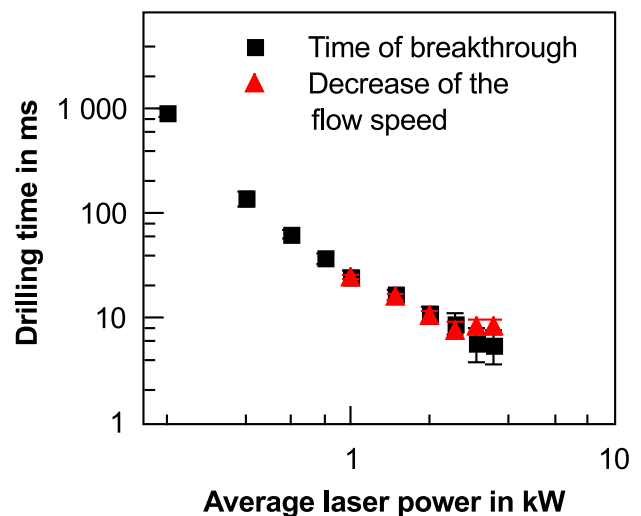

Fig. 3 Influence of the cw laser power on the flow speed of the evaporated material measured at a drilling time of 5 ms. Process parameters: $\lambda = 1030$ nm, $df \approx 300$ μm, $t_{Drill} = 5$ ms, $M^2 \approx 15$, unpolarized

Fig. 4 Process time at which the samples were drilled through (*black squares*) and at which the flow speed of the ablated vapor was detected to drop (*red triangles*) as a function of the applied cw laser power. Process parameters: $\lambda = 1030$ nm, $df \approx 300$ μm, $M^2 \approx 15$, non-polarized, sample thickness: 4.5 mm

5 Conclusion and outlook

We analyzed the gas dynamic compression shocks observed in the plume of hot ablation products that are generated during laser drilling of CFRP to determine the flow speed of the ablation products. Flow speeds of up to 3300 m/s were determined. The flow speeds measured for drilling of CFRP with a cw laser beam agree well with the ones reported for ablation with pulsed laser systems [7, 8]. A distinct kink of the flow speed over time was found to correlate with the breakthrough through the workpiece.

As shown by Fig. 5, the formation of compression shocks can also be observed during laser cutting of CFRP with a non-stationary beam. In contrast to the laser drilling process with a stationary laser beam, an elongated plume is formed exhibiting several distinct flows and with corresponding compressive shocks as highlighted with the red arrows. The compression shocks of the individual flows have different distances from the workpiece surface. As the shape of the cutting groove differs from the rotationally symmetrical nozzle, the theory above cannot be applied to this situation. In the case of vapor leaving a cutting kerf, three-dimensional effects occur and the supersonic free jets should be considered as general three-dimensional flows [8]. However, the appearance of compression shocks observed for cw laser powers exceeding 0.8 kW again indicates that the ablation products have supersonic flow speeds also during processing of CFRP with a moving laser beam. No compression shocks were observed for cw laser powers below 0.8 kW.
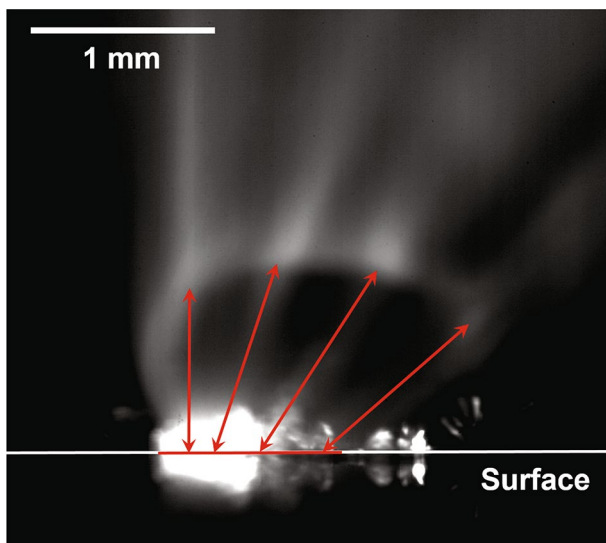
Further investigations will be required for a theoretical evaluation of the three-dimensional material flow occurring for processes with a non-stationary laser beam and to compare the resulting flow speeds with other measurement methods such as those presented in [3] where flow speeds in the range of a few hundred m/s have been reported for a continuous-wave laser cutting of carbon fiber preforms.

References

1. F.P. Bundy, W.A. Bassett, M.S. Weathers, R.J. Hemley, H.K. Mao, A.F. Goncharov, "The pressure-temperature phase and transformation diagram for carbon," updated through 1994. Carbon, **34**(2), 141–153 (1996)
2. J. Walter, M. Hustedt, R. Staehr, S. Kaierle, P. Jaeschke, O. Suttmann, L. Overmeyer, Laser cutting of carbon fiber reinforced plastics—investigation of hazardous process emissions. Physics Procedia **56**, 1153–1164 (2014)
3. P. Mucha, N. Speker, R. Weber, T. Graf, Momentum and velocity of the ablated material in laser machining of carbon fiber performs. Appl Phys A **113**, 361 (2013)
4. R. Weber, M. Hafner, A. Michalowski, T. Graf, Minimum Damage in CFRP laser Processing. Phys. Procedia. **12B**, S302 (2011)
5. R. Weber, T. Graf, P. Berger, V. Onuseit, M. Wiedenmann, C. Freitag, A. Feuer, Heat accumulation during pulsed laser materials processing. Opt. Express **22**(9), 11312 (2014)
6. T.V. Kononenko, C. Freitag, M.S. Komlenok, V. Onuseit, R. Weber, T. Graf, V.I. Konov, Heat accumulation effects in shortpulse multi-pass cutting of carbon fiber reinforced plastics. J. Appl. Phys **118**, 103105 (2015)
7. A. Narazaki, T. Sato, Y. Kawaguchi, R. Kurosaki, and H. Niino, Laser-ionization Time-of-Flight mass spectrometric studies on laser ablation of carbon fiber reinforced plastics. In: Proceeding of The second International Symposium on Laser Processing for CFRP and Composite Materials (2013)
8. M. Wiedenmann, C. Haist, C. Freitag, V. Onuseit, R. Weber, T. Graf, Ablation dynamics and shock wave expansion during laser processing of CFRP with ultrashort laser pulses. In: Proceeding Photonics West, LASE (2014)
9. D. Rist, Dynamik realer Gase. (Springer-Verlag, Heidelberg, 1996)
10. Y. Kawagushi, T. Sato, A. Narazaki, R. Kurosaki, H. Niino, Laser ablation plume from graphite and CFRP under irradiation of nanosecond UV laser pulses in air. In: Proceeding of The second International Symposium on Laser Processing for CFRP and Composite Materials (2013)
11. H. Hügel, T. Graf, Laser in der Fertigung. (Springer Fachmedien, Wiesbaden, 2014)

Fig. 5 Side view of the compression shocks in the plume generated during a laser cutting process of CFRP with a continuous-wave laser (beam moving from *right* to *left*). Process parameters: $P = 3.5$ kW, $v = 1$ m/s, $\lambda = 1030$ nm, $df \approx 300$ µm, $M^2 \approx 15$, nonpolarized